Polymeric Capsules Prepared by in Situ Synthesis and Cross-Linking of Amphiphilic Copolymer by Atom Transfer Radical Polymerization

Mir Mukkaram Ali and Harald D. H. Stöver*

Department of Chemistry, McMaster University, 1280 Main Street West, Hamilton, Ontario L8S 4M1, Canada

Received May 30, 2002; Revised Manuscript Received January 8, 2003

ABSTRACT: A technique for encapsulation of polar organic solvents using atom transfer radical polymerization (ATRP) by suspension polymerization was developed to encapsulate diphenyl ether (solubility parameter $\delta = 20.9$ MPa$^{1/2}$) for the first time. An amphiphilic terpolymer was prepared by suspension polymerization, by first preparing poly(methyl methacrylate-*co*-poly(ethylene glycol) methacrylate), P(MMA-*co*-PegMA), oligomers in solution conditions, followed by addition of a cross-linking monomer, diethylene glycol dimethacrylate, to the polymerization solution, and then transfer of this oil phase to a stirred aqueous phase. The thermodynamic requirement for encapsulation of polar core oils is that the polymer has low interfacial tensions with both the oil phase and the water phase. Therefore, increasing the polarity of the copolymer by increasing its PegMA content (0−31 mol %) led to a transition in suspension particle morphology from matrix to multihollow and hollow particles. Furthermore, particles prepared with similar monomer feed ratios by conventional free radical polymerization (CFRP) did not exhibit a multihollow structure. We attribute this difference in ATRP and CFRP suspension particle morphology to the slow rate of the ATRP reaction which allows sufficient time for diffusion of the forming polymer chains to the oil−water interface, resulting in the thermodynamically favored hollow particle morphology.

Introduction

Polymeric capsules and hollow particles can be prepared both from monomeric starting materials and from oligomers and preformed polymers.[1] In most cases, the process involves a disperse oil phase in an aqueous continuous phase, and the precipitation of polymeric material at the oil−water interface causes each oil droplet to be enclosed within a polymeric shell. Interfacial polycondensation is used to prepare poly(urea),[2] poly(amide), or poly(ester) capsules,[3] for instance, by reaction between an oil-soluble monomer and a water-soluble monomer. As well, vinyl polymers such as poly(styrene), acrylates, and methacrylates prepared by free radical polymerization under suspension[4] or emulsion polymerization[5,6] conditions have been used to prepare hollow or capsular polymer particles. In both approaches, the dispersed oil phase usually serves as the polymerization medium. The oil phase is a good solvent for the monomeric starting materials but a nonsolvent for the product polymer. Therefore, upon polymerization the system is comprised of three mutually immiscible phases. Over the past three decades, several groups have studied the factors governing the morphologies that two immiscible phases can adopt when they are brought together and confined by a third immiscible phase.[7−9]

Torza and Mason[7] studied the phase behavior of low-viscosity, immiscible organic liquids dispersed in an aqueous phase as the drops were subjected to varying shear and electric fields. They defined the spreading coefficient, $S_i = \gamma_{jk} - (\gamma_{ij} + \gamma_{ik})$, where i, j, and k represent the three immiscible phases and γ is the interfacial surface tension. For the premise that $\gamma_{12} > \gamma_{23}$, it follows that $S_1 < 0$. The definition of S_i leads to only three possible sets of values of S_i: $S_1 < 0$, $S_2 < 0$, $S_3 > 0$ [1]; $S_1 < 0$, $S_2 < 0$, $S_3 < 0$ [2]; $S_1 < 0$, $S_2 > 0$, $S_3 > 0$ [3]. For interfacial conditions of eq 1 the core−shell morphology is preferred, while for eq 2 the hemispherical morphology is preferred.[7] The theoretical predictions agree well with the experimental results. Torza and Mason used low-viscosity oils that are able to diffuse rapidly and assume the lowest interfacial energy morphology within the time frame of the experiment. Sundberg et al.[8] published a theoretical model based on the Gibbs free energy change of the process of morphology development. Starting with three immiscible phases (oil, polymer, and water), they showed that the Gibbs free energy change per unit area for the process leading to a core−shell morphology (with oil encapsulated within the polymer phase) is $\Delta G = \gamma_{op} + \gamma_{pw}(1 - \phi_p)^{-2/3} - \gamma_{ow}$, where γ_{op}, γ_{pw}, and γ_{ow} are the oil−polymer, polymer−water, and oil−water interfacial tensions and ϕ_p is the volume fraction of the polymer (in polymer plus oil "combined phase"). In the limit as ϕ_p tends to zero, $\Delta G = (\gamma_{op} + \gamma_{pw}) - \gamma_{ow}$. Thus, when $\gamma_{ow} > (\gamma_{op} + \gamma_{pw})$, the core−shell morphology with the core oil being engulfed by the polymer is the thermodynamically stable morphology. Analogous expressions were derived for the hemispherical, inverse core−shell, and distinct particle morphologies. The authors used these expressions to successfully predict the morphologies expected for a given set of interfacial conditions.

In earlier work, Berg et al.[9] showed that the above analysis is equally valid when the polymer is synthesized in situ by free radical polymerization. Poly(methyl methacrylate) was prepared via free radical polymerization by dispersing *n*-decane or hexadecane, methyl methacrylate, and an oil-soluble initiator in water containing a surfactant or stabilizer. The resultant morphology critically depended on the type of emulsifier used. The authors concluded that this was related to

* Corresponding author: e-mail stoverh@mcmaster.ca.

10.1021/ma020840t CCC: $25.00
Published on Web 03/01/2003

the minimization of interfacial energy for the particles as they are dispersed in water. In summary, the particle morphology that results from in situ polymer synthesis in suspension/emulsion polymerization conditions is predominantly driven by interfacial energy criteria.

The available studies in this area by the groups of Kasai,[10,11] Okubo,[12−18] McDonald,[5,6] and Sundberg,[8,9] all focus on encapsulation of relatively hydrophobic solvents. McDonald et al. and Sundberg et al. have encapsulated highly nonpolar core oils such as decane and octane. Kasai et al. and Okubo et al. have encapsulated slightly more polar materials such as benzene, toluene, and xylene. Since these groups set out to synthesize hollow polymer particles, the nature of the core oil has not been of relevance. However, if core−shell particles are intended for encapsulation of the core material, the technique should allow encapsulation of both hydrophobic and hydrophilic core materials.

Core−shell particles, with polymer engulfing an oil core, only form if the sum of the oil/polymer and polymer/water interfacial tensions is less than the oil/water interfacial tension. Furthermore, the polymerization conditions must permit the thermodynamic morphology dictated by the interfacial conditions to form within the time frame of the experiment. Consequently, encapsulation of more hydrophilic material demands the ability to synthesize sufficiently amphiphilic polymers that will satisfy this interfacial requirement as well as experimental conditions that allow sufficient time for the thermodynamic morphology to be reached.

We describe here the in situ ATRP synthesis of a cross-linked amphiphilic terpolymer designed to migrate to the oil−water interface yielding hollow polymer particles. The terpolymer, poly(methyl methacrylate-*co*-poly(ethylene glycol) methacrylate-*co*-diethylene glycol dimethacrylate), P(MMA-*co*-PegMA-*co*-DegDMA), was prepared by suspension polymerization by first preparing a prepolymer P(MMA-*co*-PegMA) in solution conditions, followed by addition of the cross-linking monomer, DegDMA, to the polymerization solution and transfer of this oil phase to a stirred aqueous phase. In our work, use of ATRP as the polymerization method is expected to affect both the copolymer composition and the rate at which polymer precipitates in the oil phase due to cross-linking. In addition to the usual properties of ATRP,[19,20] polymerization of cross-linking monomers by ATRP is characterized by no observable autoacceleration and by higher conversion at gel point compared to conventional free radical cross-linking polymerization.[21,22] The living nature of the ATRP polymerization and its slow rate of polymerization should have two interesting consequences when a cross-linked terpolymer based on oil-soluble and water-soluble monomers is prepared by suspension polymerization. First, ATRP should allow more time for polymer in the oil droplets to diffuse from the core to the oil water interface compared to the case of gels made via a conventional free radical polymerization. Second, even if one of the monomers partitions significantly into the water phase, it would ultimately be incorporated into forming polymer chains. The incorporation of the polar monomer into the forming polymer is important in order to satisfy the thermodynamic requirement for formation of capsular particles. Thus, the use of ATRP may have both a kinetic and a thermodynamic advantage as compared to conventional free radical polymerization.

Table 1. Solubility Characteristics of Some Organic Solvents

entry no.	solvent	solubility parameter/ $MPa^{1/2}$	solubility of solvent in water/% v/v	solubility of water in solvent/% v/v
1	ethyl acetate	18.2/18.6[a]	9 (25 °C)	4 (25 °C)
2	*n*-butyl acetate	17/17.4[a]	0.78 (25 °C)	2.9 (25 °C)
3	hexyl acetate	17.3	insoluble	insoluble
4	xylene	18.0[a]	insoluble	insoluble
5	anisole	19.4[b]	insoluble	insoluble
6	diphenyl ether	20.9[a]	insoluble	insoluble
7	dimethyl pthalate	22.1/21.9[a]	insoluble	insoluble

[a] Source: Grulke, E. A. In Solubility parameter values. *Polymer Handbook*, 4th ed.; John Wiley and Sons: New York, 1999; Table 7, p VII/688. [b] Source: Grulke, E. A. In Solubility parameter values. *Polymer Handbook*, 4th ed.; John Wiley and Sons: New York, 1999; Table 9, p VII/698.

Results and Discussion

Copolymer Synthesis in Diphenyl Ether. The ATRP synthesis of poly(methyl methacrylate-*co*-poly(ethylene glycol monomethyl ether) methacrylate)), P(MMA-*co*-PegMA), was first developed in solution polymerization conditions. Poly(methyl methacrylate) and a series of copolymers comprised of methyl methacrylate (MMA) and 9.5, 18, and 39 mol % poly(ethylene glycol monomethyl ether) methacrylate (PegMA) were prepared by solution ATRP. A copolymer containing 18 mol % PegMA was also prepared by suspension polymerization, and the molecular weights, polydispersity, and kinetics of solution and suspension ATRP were compared. The suspension copolymerization involved the ATRP synthesis of P(MMA-*co*-PegMA) oligomers under solution conditions and subsequent transfer of the oligomer solution to a stirred aqueous phase. Diphenyl ether (DPE) was used as a model polar solvent (Table 1). Furthermore, it is a good ATRP solvent owing to its low chain transfer constant, and its use for the ATRP of methacrylate monomers has been previously reported.[23]

Toluenesulfonyl chloride (TSC) was used as initiator together with a catalyst based on Cu(I)Br and 4,4′-dinonyl-2,2′-bipyridine (dNBpy). The modified bipyridine ligand ensures homogeneous catalyst solubility in diphenyl ether as well as favorable partitioning of the catalyst into the oil phase during suspension polymerizations.[24] Both the solution polymerizations and the suspension polymerizations were run at 70 °C. The aim here was to develop the ATRP synthesis of P(MMA-*co*-PegMA) for use in the encapsulation reaction, and thus the copolymerizations were carried out at low monomer loadings of 10−40 wt %. The range of interest from the encapsulation viewpoint is between 10 and 25 wt % as this amount of polymer is sufficient for constructing the capsular wall. For development of the ATRP reaction we chose a monomer feed composition of 82 mol % MMA and 18 mol % PegMA.

The experimental molecular weight (M_n(SEC)) was found to increase linearly with conversion in the 10, 25, and 40 wt % total monomer loading experiments (Figure 1). The SEC traces of the three polymerizations at 90, 96, and 99% conversion, respectively, reveal a slight high molecular weight shoulder in the 10 wt % case, while the 25 and 40 wt % polymerizations give bimodal molecular weight distributions (Figure 4). The larger discrepancy between M_n(SEC) and M_n(Theo) in the 25 and 40 wt % cases (relative to the 10 wt % case) is attributed to the high molecular weight material formed

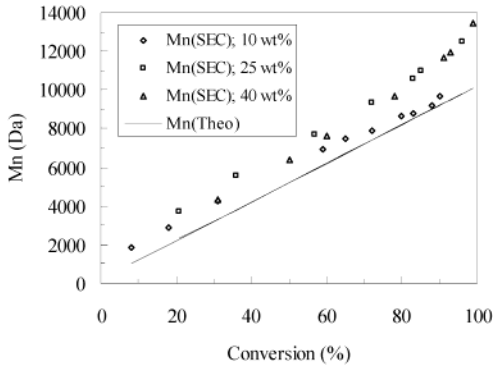

Figure 1. Plots of experimental molecular weight (M_n(SEC)) vs conversion for polymerization of P(MMA-*co*-PegMA) in DPE at 10, 25, and 40 wt % total monomer loading. $[MMA]_0$:$[PegMA]_0$:$[TSC]_0$:$[Cu(dNBpy)_2Br]_0$ = 60:14:1:1 at 70 °C.

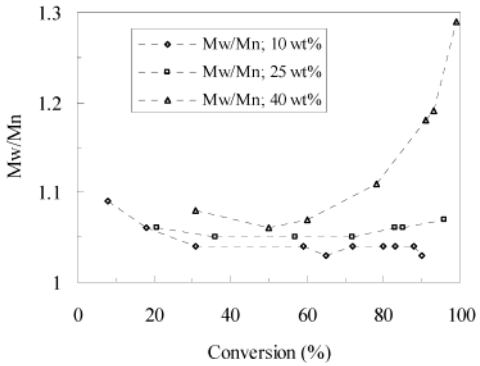

Figure 2. Plots of polydispersity index (M_w/M_n) vs conversion for polymerization of P(MMA-*co*-PegMA) in DPE at 10, 25, and 40 wt % total monomer loading. $[MMA]_0$:$[PegMA]_0$:$[TSC]_0$:$[Cu(dNBpy)_2Br]_0$ = 60:14:1:1 at 70 °C.

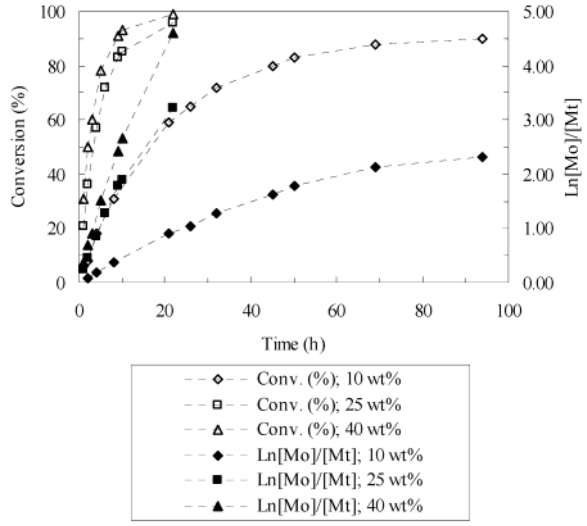

Figure 3. Kinetic profiles for polymerization of P(MMA-*co*-PegMA) in DPE at 10, 25, and 40 wt % total monomer loading. $[MMA]_0$:$[PegMA]_0$:$[TSC]_0$:$[Cu(dNBpy)_2Br]_0$ = 60:14:1:1 at 70 °C. The dotted lines connecting the data points are only meant to guide the eye.

in these cases. At 25 and 40 wt % monomer loading, the polydispersity narrowed with conversion up to about 50% conversion and then broadened continuously at higher conversions as expected for the bimodal molecular weight distributions. On the other hand, in the case of 10% monomer loading, polydispersity decreased continuously with conversion as expected for ATRP reactions (Figure 2). Figure 3 shows curvature in the

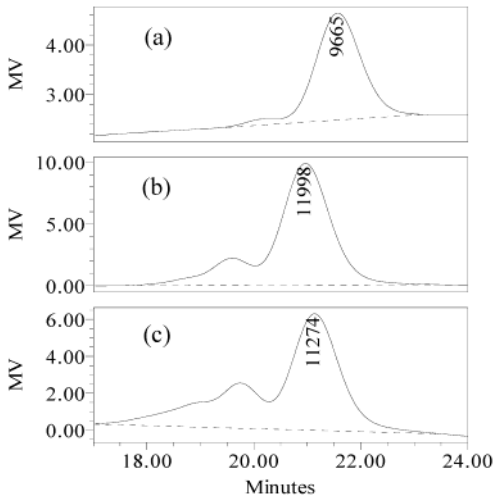

Figure 4. Size exclusion chromatographs showing the molecular weight profile of P(MMA-*co*-PegMA) containing 18 mol % PegMA at (a) 10 wt % (90% conversion), (b) 25 wt % (96% conversion), and (c) 40 wt % (99% conversion) total monomer loading in diphenyl ether at 70 °C. The reaction conditions are those presented in Figure 1.

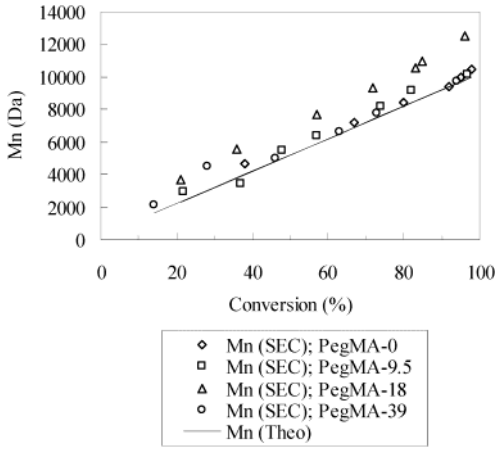

Figure 5. Plots of experimental (M_n(SEC)) and theoretical (M_n(Theo)) molecular weight vs conversion for polymerization of P(MMA-*co*-PegMA) (% PegMA = 0.0, 9.5, 18, and 39) in DPE at 25 wt %. $[TSC]_0$:$[Cu(dNBpy)_2Br]_0$ = 1:1 at 70 °C.

$\ln[M_0]/[M_t]$ vs time plots, indicating that the free radical concentration diminished with conversion in all three cases. The 10 wt % experiment showed the strongest curvature, and we propose that the polymerization kinetics are diffusion-controlled at such low monomer loading leading to the observed nonlinearity. The polymerization rate increased with monomer loading as expected (Figure 3).

Results of the ATRP synthesis of PMMA and copolymers of MMA and PegMA at constant total monomer loading of 25 wt % and containing 9.5, 18, and 39 mol % PegMA are shown in Figures 5, 6, and 7. Polymerizations proceeded to high conversions in each case, and the experimental number-average molecular weights, M_n(SEC), matched the calculated molecular weights, M_n(Theo) (Figure 5). Figure 6 shows the polydispersity profile with conversion for each of the four polymerizations. While the polydispersity decreased with conversion in the polymerization of MMA, in the copolymerizations it decreased to about 50% conversion and increased thereafter. As seen in Figure 7, the plot of $\ln[M_0]/[M_t]$ is linear in the homopolymerization but exhibits a curvature in the copolymerizations, indicating

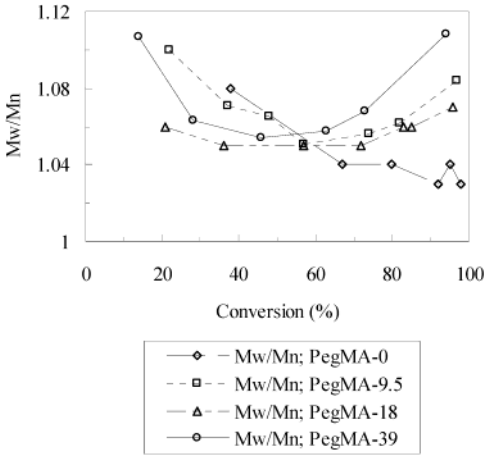

Figure 6. Polydispersity vs conversion for polymerization of P(MMA-*co*-PegMA) (mol % PegMA = 0. 9.5, 18, and 39) in DPE at 25 wt %. $[TSC]_0$:$[Cu(dNBpy)_2Br]_0$ = 1:1 at 70 °C.

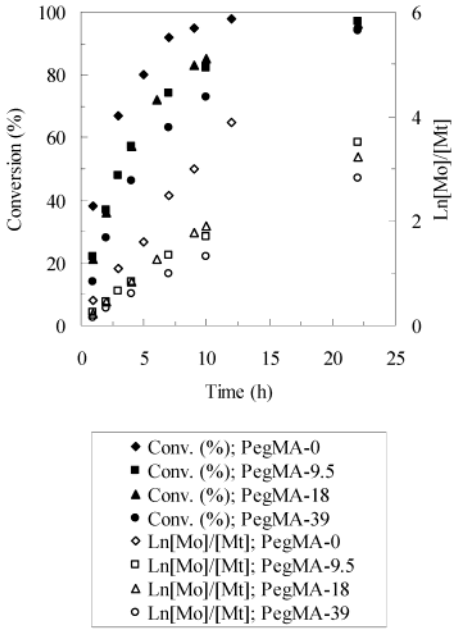

Figure 7. Kinetics of polymerization of P(MMA-*co*-PegMA) (mol % PegMA = 0, 9.5, 18, and 39) in DPE at 25 wt %. $[TSC]_0$: $[Cu(dNBpy)_2Br]_0$ = 1:1 at 70 °C.

a decrease of the radical concentration with conversion. In all three copolymerizations the polymerization medium progressively turned from brown (color of Cu(I)-$(dNBpy)_2Br$) to green (color of Cu(II)$(dNBpy)_2Br_2$), caused by accumulation of Cu(II) species. Both these observations suggest irreversible termination of polymeric radicals during polymerization.

Again, the SEC chromatograms show that while in the homopolymerization of MMA the molecular weight distribution remains monomodal throughout the polymerization, it becomes bimodal in the copolymerizations (Figure 8), and the fraction of the high molecular weight copolymer increases with increasing amounts of PegMA comonomer. The high molecular weight copolymer may result from coupling of polymeric radicals. This conforms to the observed accumulation of Cu(II) species as reaction progresses and to the drop in radical concentration with conversion as indicated by the curvature in the $\ln[M_0]/[M_t]$ vs time plots. Bimolecular coupling of polymeric radicals would result in head to head groups in the product polymer and would not contain

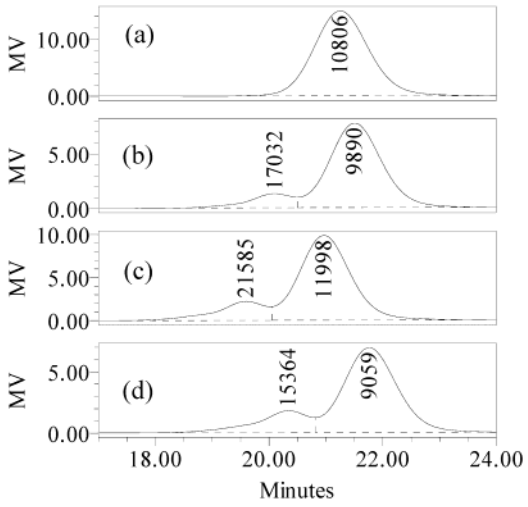

Figure 8. Size exclusion chromatographs showing the molecular weight profile of (a) PMMA at 98% conversion; P(MMA-*co*-PegMA) containing (b) 9.5% PegMA at 97% conversion, high molecular weight peak (HMWP) is 12% of total peak area; (c) 18 mol % PegMA at 96% conversion, HMWP is 17% of total peak area; and (d) 39 mol % PegMA at 94% conversion, HMWP is 20% of total peak area. The reaction conditions are those presented in Figure 5.

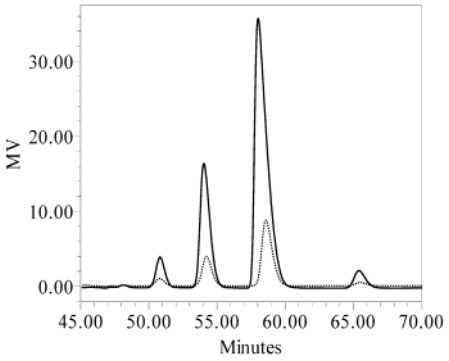

Figure 9. Aqueous size exclusion chromatographs of PegMA (a) in 2% (w/w) aqueous 0.1 M $NaNO_3$ and 100 ppm of NaN_3 (solid line) and (b) aqueous phase of PegMA partitioning experiment done at 70 °C between 80 mL of water and 20 mL of 10% (w/w) PegMA solution in diphenyl ether (dotted line). Injection volume: 30 μL. Elution solvent: aqueous 0.1 M $NaNO_3$ and 100 ppm of NaN_3. Flow rate: 0.8 mL/min. Column temperature: 35 °C. Refractive index detector temperature: 30 °C.

bromide or chloride end groups. We are in the process of checking this by NMR spectroscopy and MALDI mass spectrometry.

Partitioning of PegMA into the Water Phase. The encapsulation process involves partial synthesis of the amphiphilic terpolymer in suspension conditions. Monomer partitioning into the aqueous phase can alter the effective monomer concentration in the oil phase and directly affect the terpolymer composition and hence its polarity and morphology. MMA and DegDMA have limited water solubility; however, PegMA containing ~5 ethylene glycol units is water soluble at room temperature. The partitioning of PegMA into the water phase at 70 °C in our experimental conditions was measured by equilibrating a 10% solution of PegMA in diphenyl ether with a 4-fold excess of water, separating the two phases while still at 70 °C and determining the PegMA concentration in the water phase by aqueous size exclusion chromatography. Figure 9 shows the SEC chromatogram of a 2% PegMA solution overlaid with

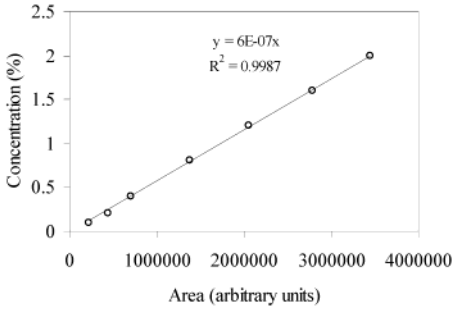

Figure 10. Aqueous size exclusion chromatography calibration curve of PegMA in water based on total area under the five component peaks. Chromatographic conditions as in Figure 7.

that of the aqueous phase of the partitioning experiment. Both chromatograms show five components. PegMA ($M_n \sim 300$ Da) (Aldrich) macromonomer consists of a mixture of compounds with an average of 4−5 ethylene oxide units in the pendant poly(ethylene glycol) monomethyl ether (Peg) chain. On the basis of the retention time in aqueous size exclusion chromatography, we assigned the five component peaks at retention times (RT) of 47.9, 50.5, 53.8, 57.7, and 65.0 min to 7, 6, 5, 4, and 3 ethylene oxide units in the pendant Peg chain. Electrospray mass spectrometry of the aqueous GPC fractions at RT = 50.5, 53.8, 57.7, and 65.0 min showed ($M + Na^+$) ion peaks at m/e = 387.2, 343.2, 299.1, and 255.0 respectively, confirming our assignment. Despite the difference in the length of the pendant Peg chain, no significant difference in the partitioning of the PegMA components between diphenyl ether and water was observed. Figure 10 therefore gives the combined PegMA calibration curve for 0.1−2% (w/w) PegMA in 0.1 M $NaNO_3$ and 100 ppm of NaN_3. This gave a combined PegMA partition coefficient, k_{water} = 0.05; i.e., 18% (w/w) PegMA partitions into the water phase in the suspension polymerizations.

Copolymer Synthesis in Suspension Conditions. Next, the ATRP synthesis of P(MMA-*co*-PegMA) was performed, in part, in suspension conditions. The purpose of this experiment was first to show that P(MMA-*co*-PegMA) can be prepared by ATRP in suspension polymerization conditions and second to confirm that the composition of the formed copolymer would reflect the comonomer feed ratio. P(MMA-*co*-PegMA) containing 18 mol % PegMA was chosen for this experiment. The copolymer synthesis was initiated in diphenyl ether in solution conditions at 70 °C and allowed to proceed to a number-average molecular weight of about 2500 Da, corresponding to about 25% conversion. At this point, the solution polymerization mixture was transferred under argon to a 4-fold excess of water (containing 1% (w/w) PVA) at 70 °C and mechanically stirred, yielding an oil in water suspension.

Results of the suspension reaction for 25% monomer loading (in diphenyl ether oil phase) are presented in Figures 11 and 12. Figure 11 shows a slight enhancement of reaction rate in the suspension polymerization compared to the solution polymerization. This is attributed to the higher partitioning of Cu(II) catalyst species into the water phase relative to Cu(I) species.[25] Plots of $\ln([M_0]/[M_t])$ vs time are nonlinear in both cases for reasons discussed above. The molecular weight increased linearly with conversion in both cases; however, the polydispersity was significantly higher in the suspension polymerization (Figure 12).

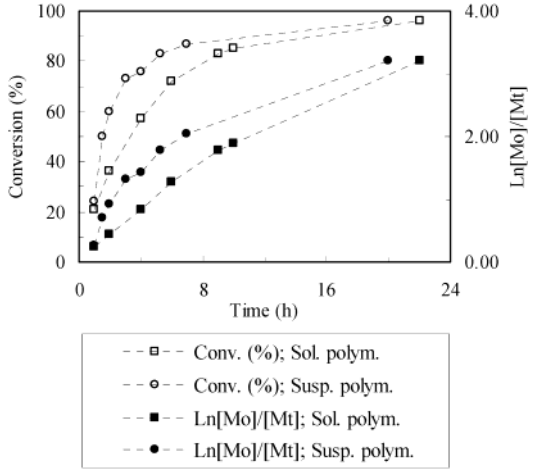

Figure 11. Kinetics of solution and suspension polymerization of P(MMA-*co*-PegMA) (18 mol % PegMA). $[MMA]_0$:$[PegMA]_0$:$[TSC]_0$:$[Cu(dNBpy)_2Br]_0$ = 60:14:1:1; 25% total monomer in DPE; oil (monomers + DPE)/water ratio in suspension = 1:4; both polymerizations at 70 °C. The dashed lines are meant only to guide the eye.

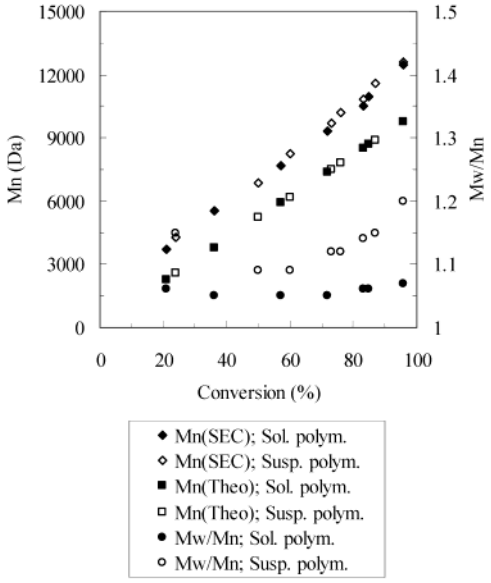

Figure 12. Plots of molecular weight and polydispersity vs conversion for solution and suspension polymerization of P(MMA-*co*-PegMA) (18 mol % PegMA). $[MMA]_0$:$[PegMA]_0$:$[TSC]_0$:$[Cu(dNBpy)_2Br]_0$ = 60:14:1:1; 25% total monomer in DPE; oil (monomers + DPE)/water ratio in suspension = 1:4; both polymerizations at 70 °C.

Higher polydispersity is consistent with higher radical concentration as this leads to more irreversible termination via radical coupling and disproportionation reactions. Like the solution polymerization product, the suspension polymerization product also contains high molecular weight material. In addition, the low molecular weight fraction has a higher polydispersity (Figure 13). This is consistent with higher radical concentrations in the suspension system.

^{13}C NMR was used to confirm that the water-soluble comonomer, PegMA, is incorporated into the growing polymer chains in the oil phase during the course of the suspension polymerization. NMR spectra of samples taken prior to, during, and at the end of the suspension polymerization were recorded. Figure 14 shows the carbon-13 spectrum and the *J*-modulated spin sort spectrum of the copolymer. The methoxy group of the

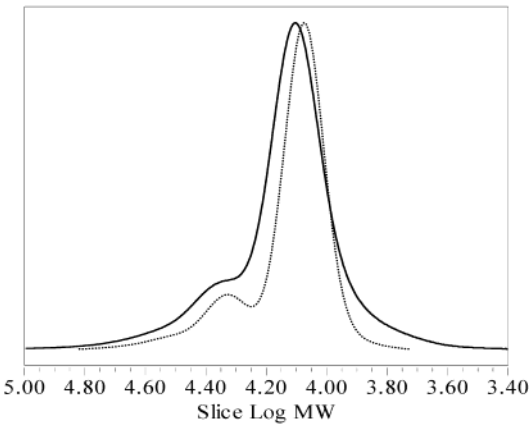

Figure 13. Molecular weight distributions of P(MMA-*co*-PegMA) (18 mol % PegMA) prepared by solution polymerization (dashed line) and suspension polymerization (solid line) both at 96% conversion. Reaction conditions are those presented in Figure 11.

MMA comonomer was assigned to $\delta_C = 51.9$ ppm, while that of the PegMA comonomer was assigned to $\delta_C = 59.2$ ppm on the basis of the expected chemical shift values. ^{13}C NMR spectra of a sample drawn just prior to transferring the organic reaction mixture to the aqueous phase, of samples from the suspension polymerization, and of the corresponding copolymer prepared by solution polymerization (conversion = 100%) were recorded. Integration of the relevant peaks indicated only 12% PegMA content in all of the spectra, while the monomer feed in both the solution and suspension polymerizations contained 18.8% PegMA. Addition of a paramagnetic relaxation agent, cr(acac)$_3$, yielded a PegMA content of 14% in both the solution polymerization and suspension polymerization samples. Finally, a gated decoupling experiment was run to reduce possible enhancement of the MMA methoxy carbon due to the nuclear Overhauser effect, and this indicated a PegMA content of 17% for both the solution polymerization and suspension polymerization samples (Figure 15). This confirms that PegMA was indeed incorporated into the copolymer to the same extent in the suspension polymerization as it was in the solution polymerization.

Encapsulation of Diphenyl Ether. The encapsulation process consisted of three steps: synthesis of low molecular weight amphiphilic copolymers by solution ATRP, addition of the cross-linking monomer to the reaction solution followed by a 10 min mixing period to ensure homogeneous distribution of the cross-linking monomer, and transfer of this oil phase to 4 times excess of 1% aqueous poly(vinyl alcohol) (PVA) in a baffled reactor. The resulting suspension was mechanically stirred with a propeller-type mixer. A series of encapsulation experiments were performed to study the effect of the polymer composition on the internal morphology of the resultant polymer particles. Table 2 gives details of these formulations. In entries 1−4, the water-soluble monomer was varied from 0 to 31 mol % while the cross-linker and the total polymer loading in the oil phase were held constant. The total polymer loading in the oil phase was held constant at 30 ± 4% (w/w) so that differences in particle morphology at a given conversion to polymer can be related directly to the interfacial properties of the forming polymer in the oil phase.

ATRP was used as the polymerization method in entries 1−4 while conventional free radical polymerization (CFRP) was used in control experiments (entries 5 and 6). Figure 16 shows an environmental scanning electron micrograph (ESEM) of the suspension polymer particles PegMA-15. The ESEM image showed that while most polymer particles maintained their spherical shape some were deflated and assumed a red blood cell like shape under the high vacuum in an ESEM sample preparation step. This suggests that the polymer particles have a hollow or less dense interior and a dense surface shell. Transmission electron microscopy (TEM) was conducted to determine the internal morphology of

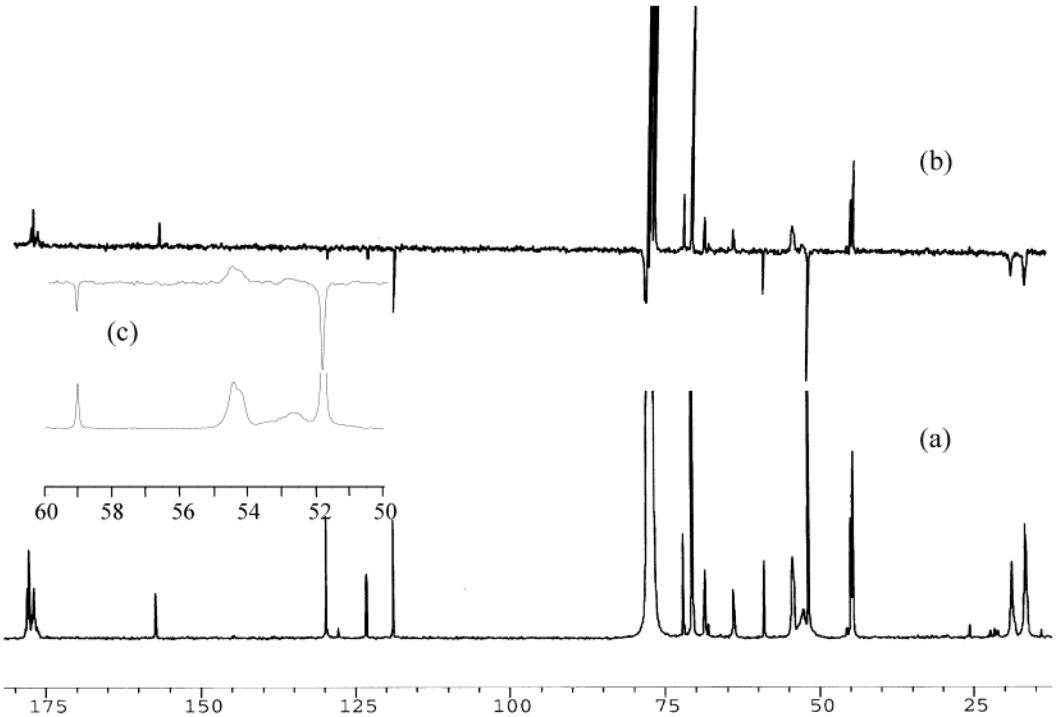

Figure 14. (a) Carbon-13 NMR of P(MMA-*co*-PegMA) in $CDCl_3$. (b) *J*-modulated spin sort spectrum of P(MMA-*co*-PegMA). (c) Expansion ($\delta_C = 50-60$ ppm) of spectra a and b.

Table 2. Reaction Conditions for Encapsulation of Diphenyl Ether[a]

expt no./ sample code	polymer loading in oil phase (% w/w)	mol % cross-linking monomer (DegDMA)	mol % water soluble monomer (PegMA)	conversion at transfer to suspension (% w/w)	final conversion to polymer (% w/w)	conversion to polymer of particles (% w/w)	internal particle morphology (TEM)[b]
1/PegMA-0	32	20	0	57	100	82	matrix
2/PegMA-8	34	20	8	35	98	83	matrix
3/PegMA-15	33	20	15	57	100	98	matrix
4/PegMA-31	31	20	31	46	99	92	capsule
5[c]/PegMA-0-C	30	20	0	0	93	93	matrix
6[d]/PegMA-31-C	28	20	31	0	98	79, 97	matrix

[a] All suspension polymerizations were carried out using a 1:4 oil/water ratio at 70 °C using 1% PVA as suspension stabilizer (unless specified otherwise). [b] Transmission electron microscopy. [c] 3% methylcellulose was used as suspension stabilizer. [d] 3% PVA was used as suspension stabilizer.

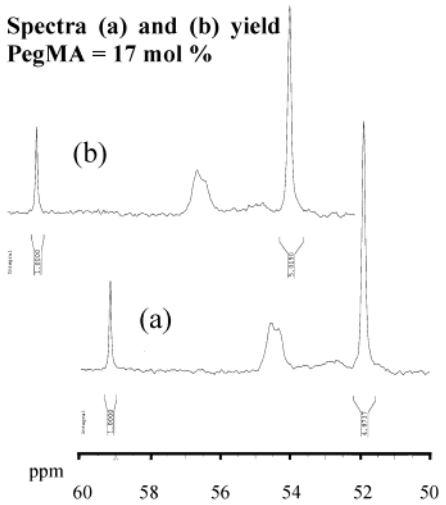

Figure 15. Carbon-13 spectra ($\delta_C = 50-60$ ppm) of P(MMA-*co*-PegMA) in $CDCl_3$ with $Cr(acac)_3$ in a gated decoupling experiment: (a) prepared by solution polymerization at 100% conversion; (b) 2 h in suspension polymerization at 82% conversion.

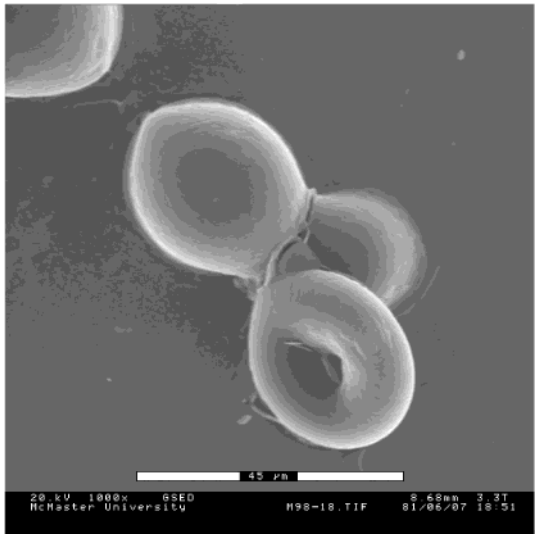

Figure 16. ESEM micrograph showing suspension polymer particles of P(MMA-*co*-PegMA) cross-linked with DegDMA. $[MMA]_0:[PegMA]_0:[DegDMA]_0:[TSC]_0:[Cu(dNBpy)_2Br]_0 = 30:7:9:1:1$; 32% total monomer in DPE; suspension = 20% monomers + DPE and 1% PVA (relative to water) at 70 °C.

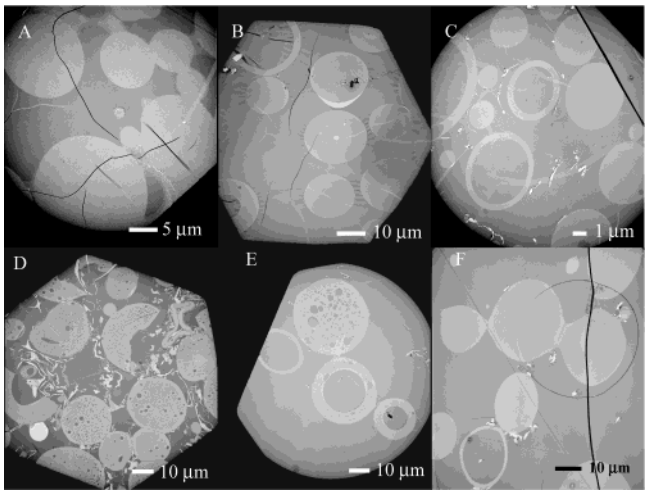

Figure 17. TEM micrographs showing internal morphology of suspension particles using DPE as oil phase: (A) PegMA-0 particles (conversion = 90%) prepared by CFRP. (B) PegMA-0 particles (conversion = 99%) prepared by ATRP. (C) PegMA-8 particles (conversion = 98%) prepared by ATRP. (D) PegMA-15 particles (conversion = 98%) prepared by ATRP. (E) PegMA-31 particles (conversion = 92%) prepared by ATRP. (F) PegMA-31 particles (conversion = 100%) prepared by CFRP.

the particles. Figure 17 presents the internal morphology of the ATRP particles and the CFRP particles. In the ATRP particles a clear transition in morphology is observed upon increasing the fraction of water-soluble monomer in the oil phase from 0 to 31 mol %. ATRP-PegMA-0 (Figure 17B) particles exhibit a matrix morphology. This suggests that PMMA cross-linked with DegDMA has no tendency to migrate to the oil water interface as it precipitates from DPE. The ATRP-PegMA-8 particles also exhibit matrix morphology, but some hollow particles are also observed. This suggests some tendency to migrate to the oil water interface, but the predominant morphology still remains the matrix morphology (Figure 17C). ATRP-PegMA-15 particles exhibit a macroporous interior, suggesting a decrease in solubility of the cross-linked terpolymer in the DPE oil phase and the resulting tendency to yield macroporous structures. In this case, the cross-linked terpolymer fills the entire volume of the suspension polymer particles; however, a macroporous interior characterized by internal voids and a relatively high density surface skin are observable. This morphology suggests that some amphiphilic terpolymer migrates to the oil−water interface; the rest remains kinetically and enthalpically trapped in the interior of the particle to form a lower density matrix. Upon further increasing the PegMA content to 31 mol % (ATRP-PegMA-31), the particles exhibit a matrix morphology characterized by large internal voids.

To study the effect of having used a living polymerization, control experiments using conventional free radical polymerization were conducted. CFRP-PegMA-0 particles and CFRP-PegMA-31 (entries 5 and 6, Table

2) particles were prepared using similar monomer compositions and polymerization conditions as the analogous ATRP particles. In these experiments, initiator, monomers, and solvent were mixed at room temperature and degassed by a stream of argon for 30 min. This oil phase was then transferred to a 4-fold excess of water containing 3% stabilizer (PVA or methyl cellulose) at 70 °C in a reactor. The colloidal suspension in CFRP-PegMA-31 experiment was stable only when 3% PVA was used. Similarly, the CFRP-PegMA-0 suspension was stable only when 3% methylcellulose was used. Thus, relative to the ATRP experiments, the CFRP suspension polymerizations needed higher viscosity of the water phase (obtained either through higher levels of PVA or through a more viscous stabilizer, methylcellulose) to yield stable suspensions. This may be due to the additional stability of the ATRP suspension caused by the presence of preformed amphiphilic copolymer in the oil droplets. The suspension was mixed at 1000 rpm for 30 min and at 500 rpm thereafter. Figure 17A,F shows the internal morphology of the suspension particles obtained. Both compositions give similar matrix type particles. Thus, there is a clear difference in morphology between the ATRP particles and the CFRP particles. ATRP of cross-linking monomers is characterized by low rates of polymerization, no observable autoacceleration, and higher conversion at gel point compared to conventional free radical cross-linking polymerization.[21,22] Since the cross-linking reaction is slow in ATRP, the forming gels phase separate from the core oil at a relatively slow rate. Thus, when the thermodynamically favored morphology is one in which the polymer engulfs the core oil, then there is more time for polymer in the oil to diffuse from the core to the oil water interface compared to gels made by the conventional free radical polymerization. Thus, the use of ATRP has a kinetic advantage as compared to conventional free radical polymerization, yielding the observed hollow particles when ATRP is used but matrix particles when CFRP is used.

Conclusions

In this work, increasing the polarity of the copolymer by increasing its PegMA content (0−31 mol %) led to a transition in suspension particle morphology from matrix to multihollow and capsular particles. In contrast, comparable suspension particles prepared by conventional free radical polymerization (CFRP) only showed matrix structure. Thus, we have shown that the use of a living/controlled polymerization characterized by slow rate of polymerization allows the thermodynamically favored morphology to be achieved within the time frame of the encapsulation experiment. This finding is particularly important for encapsulation of polar core oils because the driving force for polymer migration to oil water interface is relatively weak unless the polymer forming in the oil phase is highly polar. Preparing polar polymer in the oil phase by suspension polymerization is challenging because polar monomers are water-soluble and therefore inherently not easily adaptable to polymerization by a suspension polymerization. As well, ATRP permits preparing suspension copolymers comprised of water-soluble and oil-soluble comonomers. In ATRP the majority of the polymer chains remain alive throughout the polymerization, and so incorporation of water-soluble monomer into the forming chains continues until all monomer is consumed. In our present work because only about 20% of the PegMA comonomer was found to partition into the water phase. This advantage would be even more useful in the case of larger or more polar PegMA analogues. In future work we will explore this concept using a similar water-soluble monomer that would partition more strongly into the water phase. Since the incorporation of water-soluble monomer into the forming polymer in the oil phase is important in the encapsulation of polar core oils, the use of ATRP may then have both a kinetic and a thermodynamic advantage as compared to conventional free radical polymerization. We recognize that the presence of copper catalyst in the final suspension particles may be undesirable for certain applications. In future, use of lower concentrations of a more active catalyst or use of iron-based ATRP catalysts would address this concern. Also, our finding may be extended to any living free radical polymerization such as RAFT or nitroxide-mediated polymerizations.

Experimental Section

Materials. Toluenesulfonyl chloride (TSC) (99+%), 4,4′-dinonyl-2,2′-dipyridyl (dNBpy) (97%), diphenyl ether (DPE) (99%), and poly(vinyl alcohol) (PVA) (80% hydrolyzed, M_w = 9000−10 000 Da) were purchased from Aldrich and used as received. Methylcellulose (viscosity of 2% solution, 4000 cps) was purchased from Matheson Coleman and Bell and used as received. Copper (I) bromide (98%, Aldrich) was purified according to a published procedure.[26] Methyl methacrylate (99%), poly(ethylene glycol monomethyl ether) methacrylate ($M_n \sim$ 300 Da), and diethylene glycol dimethacrylate (95%) were obtained from Aldrich and passed over a basic alumina column to remove inhibitor. Neutral alumina and basic alumina (both Brockman Activity 1, mesh 60−325) were purchased from Fisher Scientific and used as received. Tetrahydrofuran (99%, Caledon Laboratories Limited) and pentane (98%, Caledon Laboratories Limited) were used as received.

Solution ATRP in Diphenyl Ether. CuBr (72.8 mg, 0.5 mmol), dNBpy (408.8 mg, 1.0 mmol), MMA (2060 mg, 21 mmol), PegMA (2000 mg, 16 mmol), and DPE (15 000 mg) were placed in a round-bottomed flask in a nitrogen-filled glovebag and closed with a septum. TSC (95.3 mg, 0.5 mmol) was dissolved in a portion of MMA (940 mg, 9 mmol) in a vial equipped with a septum inside a nitrogen-filled glovebag. The monomer and catalyst solution was degassed in a stream of argon for 30 min and then transferred to an oil bath at 70 °C. The initiator solution (1 mL) was introduced in one aliquot via a syringe that had been previously degassed with a stream of argon for 3 min. Samples (1 mL) were drawn periodically via a previously degassed syringe for gel permeation chromatography (GPC) and conversion measurements. GPC samples (0.2 mL) were prepared by diluting with THF (1 mL) and passing over a neutral alumina column to remove catalyst. Conversion was determined gravimetrically. This involved precipitation (twice) of 0.8 mL samples in 18−19 mL of cold pentane in 20 mL vials; the vials were then centrifuged at 3500 rpm, the supernatant was decanted, and the precipitate was vacuum-dried (at 60 °C) to constant weight. The polymerization proceeded to quantitative conversion (see Figures 1−3) with 17 mol % PegMA (by ^{13}C NMR) incorporated in the copolymer.

Suspension ATRP. A solution polymerization having the same composition as described above was initiated at 70 °C with addition of initiator solution at once in one aliquot. At 1 h reaction time (∼25% conversion) this prepolymer solution was transferred via cannula to a Buchi Miniclave Drive 100 mL glass reactor containing distilled, deionized water (80 mL, 1% (w/w) PVA) that had been previously degassed in a stream of argon for 1 h and heated to 70 °C. The reactor was equipped with appropriate baffles to break the vortex caused by mixing. The suspension was stirred mechanically at 1000 rpm for 30 min and at 500 rpm subsequently until the end of suspension

polymerization, using a propeller-type mixer. Aqueous suspension samples (5 mL) for conversion measurement and GPC analysis were drawn periodically via a syringe. These samples were then centrifuged at 3500 rpm, giving an organic bottom layer and aqueous supernatant that was carefully decanted. The wet organic layer was then freeze-dried. The freeze-dried samples, now containing diphenyl ether, unreacted monomer, and copolymer, were dissolved in THF (5 mL) by rolling the vials gently in a modified hot dog roller at room temperature for 24−48 h. The THF solutions were precipitated in pentane (15 mL), centrifuged at 3500 rpm, decanted (this sequence was carried out twice), and vacuum-dried at 70 °C to constant weight. The polymerization proceeded to 96% conversion (see Figures 7 and 8) with 17 mol % PegMA (^{13}C NMR) incorporated in copolymer.

Encapsulation of Diphenyl Ether in Cross-Linked Terpolymer. A solution copolymerization comprised of the same composition was initiated as described above. At 57% conversion the cross-linking monomer, DegDMA (2220 mg, 9 mmol), was added, and the mixture was stirred for 10 min before being transferred via cannula to a 100 mL glass reactor containing distilled, deionized water (80 mL, 1% PVA) that had been previously degassed in a stream of argon for 1 h. The reactor was equipped with a set of baffles to prevent vortexing. The suspension was stirred mechanically at 1000 rpm for 30 min and at 500 rpm subsequently until the end of suspension polymerization using a propeller-type mixer. Aqueous suspension samples (5 mL) for conversion measurement were drawn periodically by syringe. The suspension samples were freeze-dried. The freeze-dried samples, now containing diphenyl ether, unreacted monomer, and cross-linked terpolymer, were swollen in THF (5 mL) by rolling the vials gently in a modified hot dog roller at room temperature for 24−48 h. The swollen particles were precipitated in pentane (15 mL), centrifuged at 3500 rpm, decanted (this sequence was done twice), and vacuum-dried at 70 °C to constant weight. The conversion to cross-linked polymer was 100%. The morphology of the cross-linked particles is shown in Figure 17. To determine conversion to particles, the precipitated polymer particles that contain both sol and gel fractions were swollen in 18−19 mL of THF by rolling in a hot dog roller for 12−24 h and then centrifuged at 3500 rpm. The supernatant was decanted. This procedure was repeated twice before the gel fraction was vacuum-dried to constant weight at 60 °C. Conversion to gel fraction was 98%.

Measurements. The identities of the components in poly(ethylene glycol monomethyl ether) methacrylate macromonomer were confirmed by positive ion electrospray mass spectrometry using a triple quadrapole Micromass Ultima instrument. Polymer molecular weight was determined by size exclusion chromatography using a Waters 515 HPLC pump connected to three Waters 5 μm (7.8 × 300 mm) Styragel (HR2, HR3, and HR4) linear columns (exclusion limits 500−20 000, 500−30 000, and 5000−600 000 Da) and a Waters 2414 refractive index detector. The HPLC pump was equipped with a Water 717 plus Autosampler and computer controlled using the Millenium 32 Chromatography Manager. The column and detector temperature were set at 40.0 and 35.0 °C, respectively. Tetrahydrofuran was used as elution solvent (flow rate = 1 mL/min), and narrow disperse linear polystyrene standards were used for calibration. The surface and internal morphologies were determined using a Phillips-2020 environmental scanning electron microscope (ESEM) and a JEOL 1200EX transmission electron microscope (TEM), respectively. ESEM samples were prepared by depositing dilute aqueous dispersions of polymer particles on cover glass slips fixed to aluminum stubs, drying at room temperature, and sputter-coating with a 5 nm layer of gold. For TEM analysis, polymer particles were embedded in Spurr epoxy resin and microtomed to ∼100 nm thickness. Optical microscopy was performed using an Olympus BH-2 microscope, equipped with a Kodak DC 120 digital camera. The ^{1}H and ^{13}C NMR spectra were recorded in $CDCl_3$ at 300 and 75 MHz, respectively, on a Bruker AV-300 instrument.

Acknowledgment. We acknowledge NSERC and 3M Canada for funding this research and Dr. Nicholas Burke and Wen Hui Li for valuable suggestions. We also thank Lisa M. Croll and Anna Shulkin for their help with electron microscopy.

References and Notes

(1) Arshady, R. *Microspheres, Microcapsules Liposomes* **1999**, *1*, 1461−1732.
(2) Beestman, G. B.; Deming, J. M. U.S. Patent 4,417,916, 1983.
(3) Arshady, R. *J. Microencapsulation* **1989**, *6*, 13−28.
(4) Kasai, K.; Hattori, M.; Takeuchi, H.; Sakurai, N. U.S. Patent 4,908,271, 1990.
(5) McDonald, C.; Chonde, Y.; Cohrs, W. E.; MacWilliams, D. C. U.S. Patent 4,973,670, 1990.
(6) McDonald, C. J.; Bouck, K. J.; Chaput, A. B.; Stevens, C. J. *Macromolecules* **2000**, *33*, 1593−1605.
(7) Torza, S.; Mason, S. G. *J. Colloid Interface Sci.* **1970**, *33*, 67.
(8) Sundberg, D. C.; Casassa, A. P.; Pantazopoulos, J.; Muscato, M. R. *J. Appl. Polym. Sci.* **1990**, *41*, 1425.
(9) Berg, J.; Sundberg, D.; Kronberg, B. *J. Microencapsulation* **1989**, *6*, 327.
(10) Kasai, K.; Hattori, M.; Takeuchi, H.; Sakurai, N. US Patent 4,798,691, 1989.
(11) Itou, N.; Masukawa, T.; Ozaki, I.; Hattori, M.; Kasai, K. *Colloids Surf. A: Physiochem. Eng. Aspects* **1999**, *153*, 311−316.
(12) Okubo, M.; Minami, H.; Yamashita, T. *Macromol. Symp.* **1996**, *101*, 509−516.
(13) Okubo, M.; Minami, H. *Colloid Polym. Sci.* **1996**, *274*, 433−438.
(14) Okubo, M.; Minami, H. *Colloid Polym. Sci.* **1997**, *275*, 992−997.
(15) Okubo, M.; Konishi, Y.; Minami, H. *Colloid Polym. Sci.* **1998**, *276*, 638−642.
(16) Okubo, M.; Konishi, Y.; Minami, H. *Colloid Polym. Sci.* **2000**, *278*, 659−664.
(17) Okubo, M.; Konishi, Y.; Minami, H. *Colloid Polym. Sci.* **2001**, *279*, 519−523.
(18) Okubo, M.; Konishi, Y.; Inohara, T.; Minami, H. *Macromol. Symp.* **2001**, *175*, 321−328.
(19) Patten, T. E.; Matyjaszewski, K. *Acc. Chem. Res.* **1999**, *32*, 895−903.
(20) Patten, T. E.; Xia, J.; Abernathy, T.; Matyjaszewski, K. *Science* **1996**, *272*, 866−868.
(21) Yu, Q.; Zeng, F.; Zhu, S. *Macromolecules* **2001**, *34*, 1612−1618.
(22) Jiang, C.; Shen, Y.; Zhu, S.; Hunkeler, D. *J. Polym. Sci., Part A: Polym. Chem.* **2001**, *39*, 3780−3788.
(23) Wang, J.; Grimaud, T.; Matyjaszewski, K. *Macromolecules* **1997**, *30*, 6507−6512.
(24) Gaynor, S. G.; Qiu, J.; Matyjaszewski, K. *Macromolecules* **1998**, *31*, 5951−5954.
(25) Qiu, J.; Pintauer, T.; Gaynor, S. G.; Matyjaszewski, K.; Charleux, B.; Vairon, J. P. *Macromolecules* **2000**, *33*, 7310−7320.
(26) Keller, R. N.; Wycoff, H. D. *Inorg. Synth.* **1946**, *2*, 1.

MA020840T